Dalton Transactions

ROYAL SOCIETY OF CHEMISTRY

PAPER

View Article Online
View Journal | View Issue

Check for updates

Cite this: *Dalton Trans.*, 2024, **53**, 13142

Oxochlorin frameworks confining a β-hydroxyketone moiety†

Nivedita Chaudhri,*[a,b] Matthew J. Guberman-Pfeffer,[c] Matthias Zeller[d] and Christian Brückner*[a]

Received 11th May 2024,
Accepted 15th July 2024

DOI: 10.1039/d4dt01386g

rsc.li/dalton

Nominally, *meso*-hydroxyoxochlorins, like known 5-hydroxy-7-oxo-octaethylchlorin (**9**), its nickel complex [5-hydroxy-7-oxo-octaethylchlorinato]nickel(II) (**9Ni**), or the novel 5-hydroxy-7,17-dioxo-octaethylbacteriochlorin (**10**), incorporate an acetylacetonate (acac)-moiety in the enol form in their chromophore structures. X-Ray diffraction studies of the compounds show the presence of a strong H-bond between the enol and flanking β-ketone. Like acac, the functionality can be deprotonated. However, unlike regular acac-like moieties, we did not find any indication that this functionality is competent in chelating any of the 3d or 4d transition metal ions tested. Evidently, the conjugation that contributes to the stability of acac as a ligand cannot be expressed in the *meso*-hydroxyoxochlorins since it would perturb the aromaticity of the porphyrinic chromophores; in other words, the metal binding energies do not offset the loss in aromaticity. The halochromic properties of the molecules provide some more insight into the location of the protonation/deprotonation sites. The interpretation of the findings is supported by computations.

Introduction

The anionic form of pentane-2,3-dione **1H**, acetylacetonate (acac), is a long-known and excellent mono-anionic, bidentate *O*,*O*-ligand for a range of metal ions, forming complexes such as **1M** in which the ligand and ligand-to-metal bonds are fully conjugated (Scheme 1).[1] The chelating ability is due to the CH-acidic nature of the methylene group in **1H** and the conjugation-induced high stability of its H-bonded enol tautomer or metal ion chelate.[1a]

The chemistry of the acac ligand and 1,3-diketones,[2] in general, is well-studied.[1b] 1,3-Diketone moieties are also of relevance to a range of technical and biomedical fields.[1b,d,3] A variety of natural and nature-derived compounds are also known that bind metal ions using acac-like motifs within their frameworks.[2,3]

Porphyrins (and related porphyrinoids)[4] are excellent chelators for a wide range of metal ions in their own right.[5] Porphyrins typically act as dianionic square planar N_4-donors, forming metalloporphyrins, with the metal ions coordinated to the central cavity of the porphyrin in several in-plane and out-of-plane architectures (that may also include additional axial ligands).[4b,5,6] Expanding these classic porphyrin chelates, the last decades saw the emergence of examples of porphyrin derivatives that directly coordinate to metal ions with porphyrin framework atoms in many modalities,[7] or that carry functionalities at the outside of the macrocycle that are suited to bind metal ions.[4b,7,8] Examples include enaminoketone chelate **3** [9] and N-confused porphyrin complex **4**.[10] We primarily reference here only those porphyrin modifications that directly affect the porphyrinic π-system and ignore the many examples of chelates that were attached at more remote sites, such as the *meso*-aryl groups (Fig. 1).[7,11]

The attraction of these modified porphyrin systems is that coordination of the metal can be expected to induce large changes in the electronic properties of the chromophore,

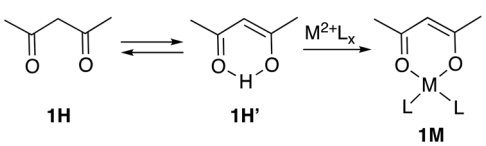

Scheme 1 The structure of pentane-2,3-dione **1H** in its two tautomeric forms, and its bidentate metal complex **1M**.

[a]*Department of Chemistry, University of Connecticut, Storrs, CT 06269-3060, USA. E-mail: c.bruckner@uconn.edu*
[b]*Department of Chemistry, Guru Nanak Dev University Amritsar, Punjab-143005, India*
[c]*Department of Chemistry and Biochemistry, Baylor University, One Bear Place #97348, Waco, Texas 76706, USA*
[d]*Department of Chemistry, Purdue University, 560 Oval Drive, West Lafayette, IN 47907-2084, USA*

†Electronic supplementary information (ESI) available: Reproductions of all spectra (UV-vis, Fl, ^{1}H, ^{13}C NMR spectra, FT-IR, MS spectra) of **10**; spectroscopic data of known compound **9** for comparison; details to the single crystal X-ray structure analyses; graphical representations of the computational data, including movies of trajectories; computational datasets. CCDC 2340919 and 2340920. For ESI and crystallographic data in CIF or other electronic format see DOI: https://doi.org/10.1039/d4dt01386g

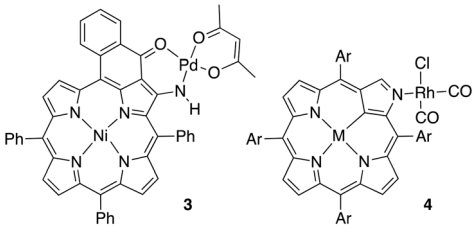

Fig. 1 Enaminoketone chelate **3** and N-confused porphyrin **4** coordinating at their functionalized periphery to metal ions.

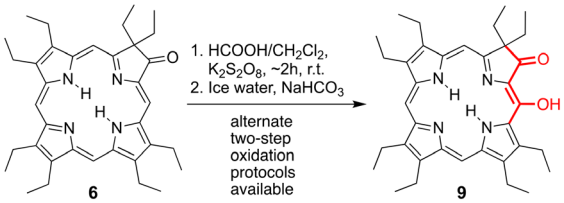

Scheme 3 Synthesis of known compound *meso*-hydroxy-β-oxochlorins **9**,[19h,20a,b] along a modified procedure.[19h] The acac-moiety is shown in red.

making these systems potentially good optical chemosensors.[12] Targeted applications in the past for porphyrins coordinating externally to metal ions were also, for instance, the generation of porphyrin assemblies for energy transfer arrays[13] or to electronically link two metal centers through a redox non-innocent porphyrinic π-system to modify their catalytic properties.[14]

The introduction of oxo-functionalities into the β-positions of the porphyrinic chromophore is one way to functionalize its periphery; this also strongly affects its electronic properties.[15] One method to introduce β-oxo functionalities into β-alkylporphyrins, such as octaethylporphyrin (**5**, OEP), is their treatment with H_2O_2 in conc. H_2SO_4 (Scheme 2).[15a,16] Harking back to the 1930's,[17] this reaction has evolved since.[15a,16,18] As a result, many aspects of the synthesis, structure, coordination, chemical and physical properties of the mono- (**6**), di- (**7**), and tri-oxochlorins (**8**) are now well-understood.[15f,16b,19]

A range of functionalization reactions of oxochlorin **6** were reported.[15a,19h,20] Most important in the context of this contribution, three independent reports described the two-step oxidation of β-oxochlorin **6** to produce *meso*-hydroxylated derivative **9**, with the *meso*-hydroxy group located adjacent to the oxo-functionality (Scheme 3).[19h,20a,b] Other isomers of the *meso*-hydroxyoxochlorins have also become known, but these carry the *meso*-hydroxy functionality at remote positions from the β-oxo-functionality.[20a,b]

At first glance, the *meso*-OH-β-ketone of compound **9** appears to be the enol form of an acetylacetone-like ligand, implying it could also coordinate metal ions, possibly even with direct electronic signaling of the binding event into the porphyrinic chromophore (Scheme 4). No study to date investigated the metal binding ability of the external *meso*-OH-β-ketone moiety. This report tests this metal binding hypothesis on **9**, its inner nickel(II) complex **9Ni**, and a related, novel dioxo-derivative **10**.

Alas, we found neither of the compounds to chelate 3d or 4d metal ions with their 'acac-like' moiety under any of the standard conditions tested. Using experiments and computations, we dissect the degree to which the typical excellent metal ion coordination properties of the acac moiety are severely compromised when embedded in a porphyrinic framework. However, we also noted that the *meso*-OH-β-ketone moieties in all *meso*-OH-β-ketone compounds have a major influence on their halochromic properties. We thus describe in more detail these properties and, supported by computations, the likely sites for the (de)protonation events.

Results and discussion

Syntheses of *meso*-OH-oxochlorins 9, its nickel(II) complex 9Ni, and *meso*-OH-dioxobacteriochlorin 10

We prepared known *meso*-OH-oxochlorin **9** [15a,16a] by slight procedural modification (change of solvent from formic acid to a mixture of CH_2Cl_2/formic acid) of the two-step functionalization procedure of oxochlorin **6** reported earlier by our group (in 25% yield over two steps, at a 100 mg-scale) (Scheme 3).[19h] Insertion of nickel(II) under somewhat forcing conditions reflecting the reduced basicity of oxochlorins compared to regular chlorins or porphyrins[15f] yielded the corresponding nickel(II) complex **9Ni** (Scheme 4).

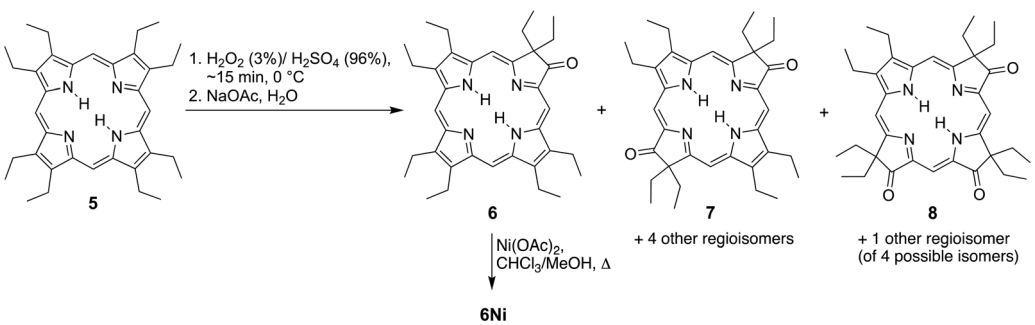

Scheme 2 Literature-known synthesis of oxochlorins by H_2O_2/H_2SO_4-mediated oxidation of octaethylporphyrin.[15a,16,18]

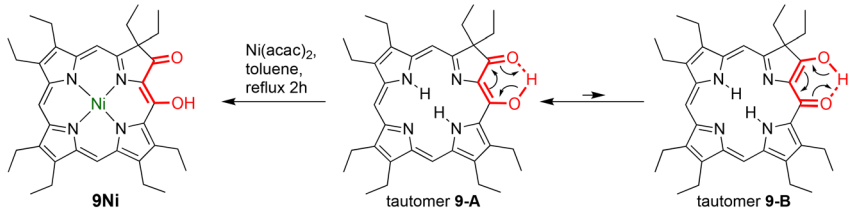

Scheme 4 Synthesis of [5-hydroxy-7-oxochlorinato]nickel(II) **9Ni** and possible tautomeric equilibrium exhibited by free base 5-hydroxy-7-oxochlorin **9** (as a representative example).

In due course of our work to oxidize a number of dioxobacteriochlorins and dioxoisobacteriochlorins using H_2O_2/H_2SO_4 to form the corresponding trioxopyrrocorphin isomers,[21] we found that treatment of dioxobacteriochlorin isomer **7** produced, next to a target triketone, a small fraction (~1.5% yield) of a non-polar product (Scheme 5). This was identified spectroscopically, by HR-MS, and by single crystal X-ray diffractometry (see below) as 5-hydroxy-7,17-dioxobacteriochlorin **10**, the dioxobacteriochlorin analogue to oxochlorin derivative **9**. While we did not isolate an isomeric product, the reaction also produced several other as yet to be identified minor fractions. Thus, the degree to which the *meso*-hydroxylation reaction of **7** is regioselective remains to be determined.

Optical properties of *meso*-OH-oxochlorin 9 and *meso*-OH-dioxobacteriochlorin 10

The UV-vis spectra of *meso*-hydroxy-β-oxo compounds **9** and **10** are both chlorin-like, with the spectrum of the dioxobacteriochlorin **10** being significantly red-shifted when compared to that of oxochlorin **9** (Fig. 2). Both compounds are emissive, with the small Stokes shift typically observed for porphyrinic chromophores. Overall, the UV-vis absorption and fluorescence emission spectra of both compounds are broadly similar to those of the parent oxo- and dioxo-chromophores **6** and **7**, respectively.[16b]

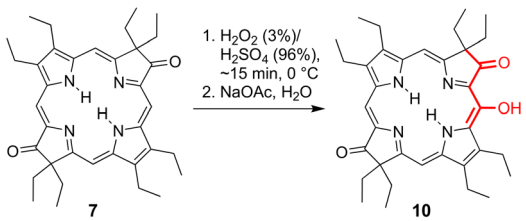

Scheme 5 Synthesis of 5-hydroxy-7,17-dioxobacteriochlorin **10** by oxidation of the parent 7,17-dioxobacteriochlorin **7**.

Scheme 4 shows the possible tautomeric structures of compound **9** that its β-hydroxy ketone moiety may allow (an equivalent tautomeric equilibrium can be proposed for compound **10**). Related keto–enol tautomeric pairs of *meso*-hydroxy-porphyrins play an important role in heme catabolism.[22] Ketone tautomer **9-B** corresponds to a macrocyle-non-aromatic oxophlorin. It is therefore expected to possess very different electronic spectra compared to chlorin-type enol tautomer **9-A**.[23] However, the finding that the *meso*-hydroxylated compounds **9** and **10** possess optical spectra that are very similar to those of the parent compounds indicates that presence of the *meso*-OH functionality affects the electronic properties of the macrocycle chromophores only to a minor degree. This further suggests that oxophlorin-type tautomeric form **9-B** (or the equivalent form for **10**) are unlikely major contributors to their electronic spectra.[23] FT-IR data of **9** and **10** also support this interpretation. In fact, the finding of compound **9** existing exclusively in the *meso*-hydroxy tautomer was already noted by Inhoffen and Gossauer on the basis of IR-spectroscopic data[20a] and Isaak, Senge, and Smith[20b] and Senge and Smith[24] based on a range of spectroscopic data. We now find that adding a

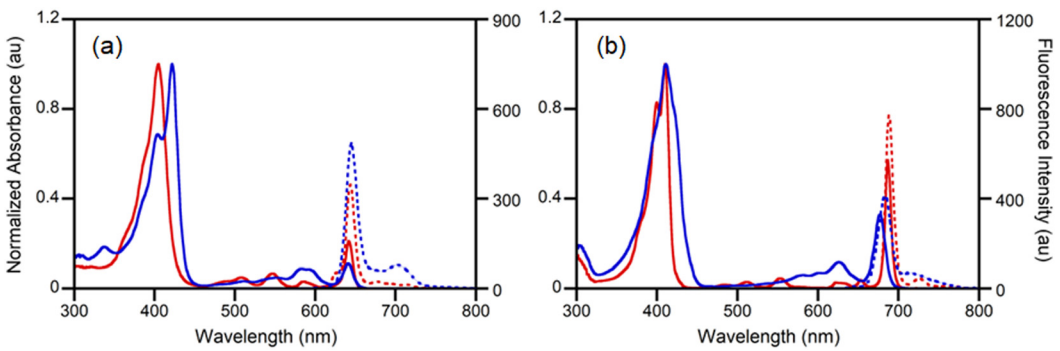

Fig. 2 UV-vis (CH_2Cl_2, solid traces) and fluorescence (CH_2Cl_2, dotted traces) spectra of (a) 7-oxochlorin **6** (red trace), 5-hydroxy-7-oxochlorin **9** (blue trace), and (b) 7,17-dioxobacteriochlorin **7** (red trace) and 5-hydroxy-7,17-dioxobacteriochlorin **10** (blue trace).

second ketone moiety to the framework of **9**, generating compound **10**, does not principally change this picture.

A computational comparison of the relative stabilities of the two possible tautomers also indicated that the *meso*-hydroxy tautomer in free base **9** or its nickel complex **9Ni** is preferred by about 10 kcal mol^{-1} (for details, see ESI†). The *meso*-OH group is computed to express an H-bond to the neighboring ketone functionality, as shown by the diagnostically short bond distances calculated and the skip-rope shape of the energy profile of a computed rotation of the –OH bond along the C_{meso}–OH bond axis, with a distinct minimum in the energy for the conformation that maximizes the H-bond interaction (see ESI†).

X-Ray structures of [*meso*-OH-oxochlorinato]nickel(II) 9Ni and *meso*-OH-dioxobacteriochlorin 10

We were able to structurally characterize compounds **9Ni** and **10**, confirming their *meso*-OH-β-oxochlorin-type connectivities with, and as spectroscopically deduced,[19h,20a,b] short, strong H-bonds between the oxygen functionalities (donor–acceptor distances of 2.69 and 2.56 Å, and hydrogen-acceptor distances of 1.84 and 1.78 Å for **9Ni** and **10**, respectively) (Fig. 3). This short distance is commensurate with the presence of a hydrogen bond.[25]

A comparison of the macrocycle conformation of **9Ni** to that of the parent non-*meso*-hydroxylated compound **6Ni**, reported previously,[20d] using a normal mode structural decomposition (NSD) analysis,[5b] shows the structural effects of introducing a *meso*-OH group (Fig. 3A). The parent compound **6Ni** exhibits two conformations in the same crystal: a largely ruffled, much non-planar, conformation (**6Ni**-non-planar) that is most typical for many nickel(II) porphyrins and chlorins and a much less distorted, primarily saddled conformation (**6Ni**-planar) that is less common, but also routinely observed.[5b] In comparison, *meso*-hydroxylation, likely through the H-bond-enforced planarization of the *meso*-OH-β-ketone motif, leads to an unusually pronounced saddled conformation of the macrocycle, with negligible contributions of other deformation modes.

The conformation of free base *meso*-hydroxylated compound **10**, in comparison to its parent compound **7** reported previously,[16b] shows that the small saddling and ruffling deformations of dioxobacteriochlorin **7** are further reduced upon *meso*-hydroxylation (Fig. 3B); the macrocycle is idealized planar. This planarity supports well the intramolecular H-bond between the *meso*-OH group and the adjacent β-ketone functionality.

Metal coordination properties of the external 'acac-moiety' of *meso*-OH-oxochlorins 9 and 9Ni, *meso*-OH-dioxobacteriochlorin 10

One enticing potential of the acac-like *meso*-OH-β-ketone functionality on compounds **9**, **9Ni**, or **10** is that metal coordination would shift the keto-enolate equilibrium to form spectroscopically distinct species upon metal coordination, forming the basis for the realization of sensitive optical metal ion sensors.[26] However, the addition of methanolic solutions of a range of 3d-transition metal ions (Ni^{2+}, Cu^{2+}, Zn^{2+}, as their acetates) or 4d metals (Pd^{2+} acetate or chloride, Ag^{+} acetate, Cd^{2+} chloride) to **9**, **9Ni**, or **10** in the absence or presence of amine bases (Et_3N, pyridine) at ambient temperature did not alter their optical spectra in any substantial fashion. Likewise, ESI^{+} mass spectrometry of these solutions also did not suggest the formation of any complexes. Warming the methanolic

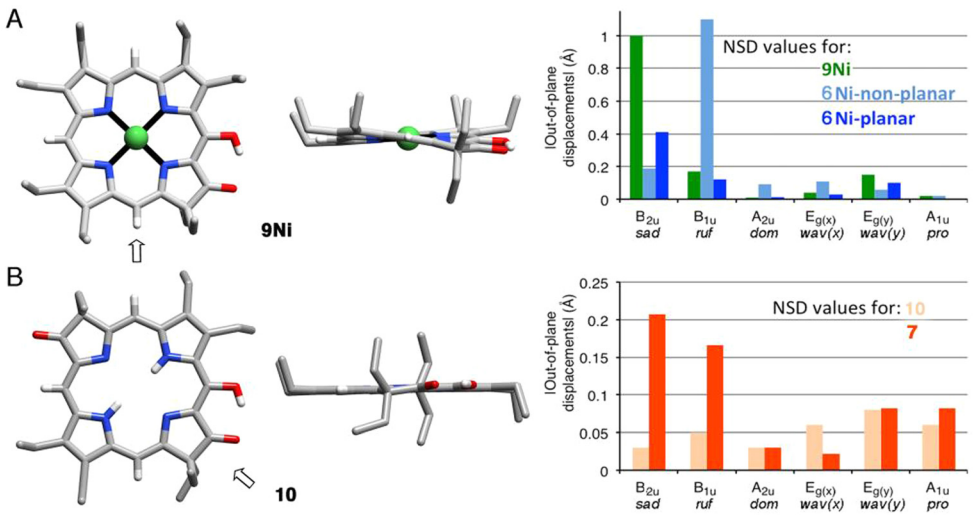

Fig. 3 Stick representation of the X-ray single-crystal structure of (A) **9Ni** and (B) **10**, top and side views (left and middle, columns, respectively); arrow in the top view image shows the point of view of the side view. All disorder and solvents (if present) are removed for clarity, as were all ethyl-hydrogen atoms. Right column: NSD analyses as implemented by Kingsbury and Senge of **9Ni** [20d] and **10**,[5b] compared to the conformation of their non-*meso*-hydroxylated parent compounds **6Ni** and **7**, respectively. For details of the structural determinations and structural analyses, including the atom numbering scheme, see ESI.†

solutions or heating DMF solutions of **9Ni** up to 90 °C over up to 24 h with select metal salts (for Cu^{2+} and Ag^{+} acetate and Pd^{2+} acetate and chloride) did not lead to the formation of a distinct complex; instead, slow decomposition were observed. In fact, when we formed nickel complex **9Ni** by reaction of free base **9** with nickel(II) ions, we already noticed the conspicuous absence of any observations that might have suggested that a peripheral nickel complex had formed.

The power of the acac-moiety as a chelate in part lies in its resonance-stabilization.[1a] In that regard, the near-exclusive presence of only the enol tautomer and thus implied absence of any resonance for the 'acac-moiety' embedded in the oxochlorins does not bode well for metal coordination. Evidently, the loss of aromaticity in the boundary oxophlorin-type resonance form is not sufficiently compensated by the energetics of the metal–ligand interactions. Thus, compounds **9**, **9Ni**, or **10** and, by extension, similar *meso*-OH-β-oxochlorins cannot be used for metal binding/sensing applications.

Halochromic properties of the *meso*-OH-oxochlorins 9 and 9Ni and *meso*-OH-dioxobacteriochlorin 10

In due course of the assessment of the reactivity of the 'acac-moiety' of the *meso*-OH-oxochlorins, we investigated their acid–base properties. One of the characteristic properties of the acac moiety is its acidity.[1a] We probed the acidity of *meso*-hydroxy-oxochlorin **9** and its nickel complex **9Ni** (in CH_2Cl_2) by UV-vis spectrophotometric titration with tetrabutylammonium hydroxide (1 M TBAOH, in MeOH). Upon addition of TBAOH, the Soret band of **9** was slightly reduced in intensity and red-shifted; its Q-band region broadened and red-shifted significantly, also (Fig. 4); its nickel complex **9Ni** showed qualitatively the same response. In comparison, the non-hydroxylated free base oxochlorin **6** was previously shown to be entirely inert to the same base conditions.[15f] Thus, the changes seen in **9**/**9Ni** can be attributed to a deprotonation of the *meso*-OH group and not to, for example, deprotonation of the NH protons.

Indeed, computations also accurately predicted the UV-vis spectra of the species $[\mathbf{9}\text{-}H^{+}]^{-}$ and $[\mathbf{9Ni}\text{–}H^{+}]^{-}$ deprotonated at the *meso*-OH group (see ESI†). Computations also put the thermodynamic preference of OH-deprotonations *versus* NH deprotonation at 12 kcal mol^{-1} (see ESI†). Furthermore, computations also predicted minimal, if any, shifts of the *meso*-protons in their ^{1}H NMR spectra, a prediction also supported by experiment (in $CDCl_3$ with TBAOH in MeOH; see ESI†). These findings are all indications that non-aromatic phlorin-like resonance structures are not any major contributor to the *meso*-oxygen-centered mono-anionic species.

We also probed the acidity of *meso*-hydroxy-dioxobacteriochlorin **10** (in CH_2Cl_2) by UV-vis spectrophotometric titration with tetrabutylammonium hydroxide (1 M TBAOH, in MeOH). Upon the addition of TBAOH, the Q-band region of **10** broadened and red-shifted significantly, and its Soret band was much reduced in intensity (Fig. 5). In comparison, the corres-

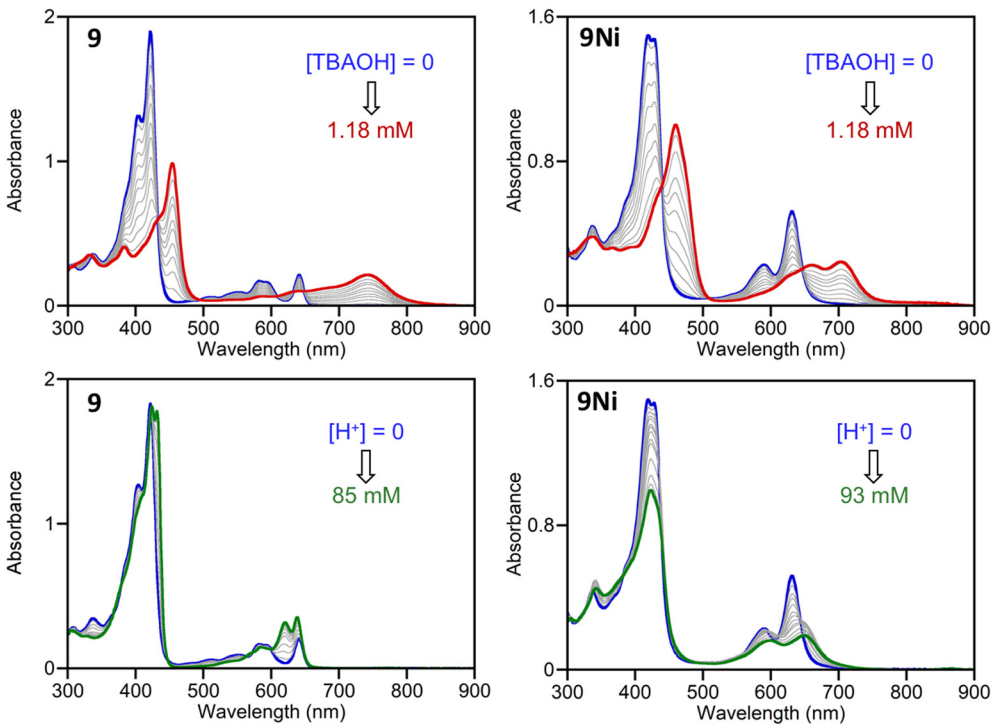

Fig. 4 UV-visible titrations (CH_2Cl_2 at 298 K) of (top row) *meso*-hydroxy-oxochlorin **9** (6.03×10^{-5} M) and its nickel complex **9Ni** (0.82×10^{-5} M) with tetrabutylammonium hydroxide (1 M in CH_3OH) in the [TBAOH] range indicated and (bottom row) *meso*-hydroxy-oxochlorin **9** (6.03×10^{-5} M) and its nickel complex **9Ni** (0.82×10^{-5} M) with TFA (CH_2Cl_2 at 298 K) in the [TFA] range indicated.

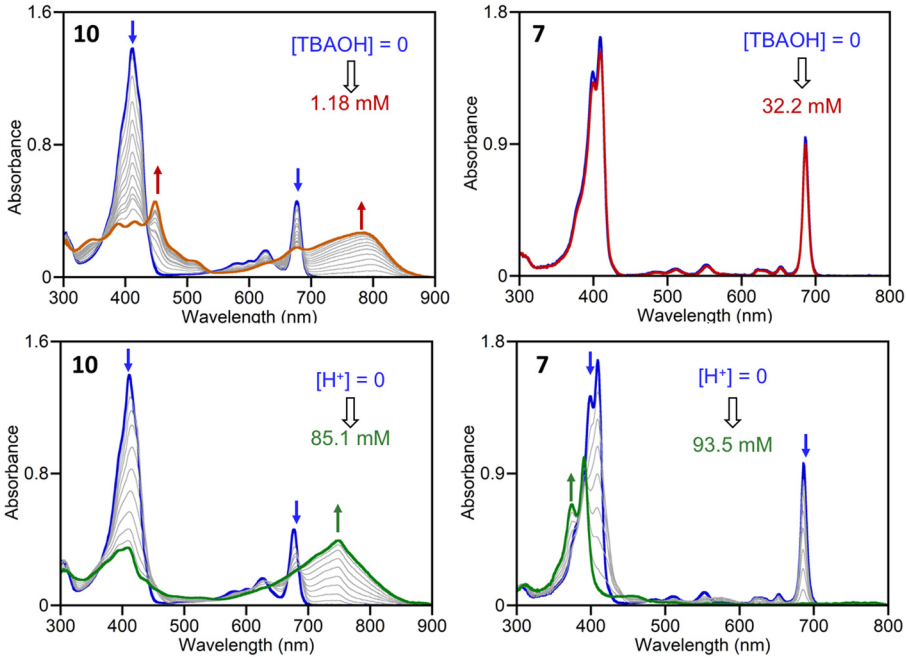

Fig. 5 UV-visible titration (CH_2Cl_2 at 298 K) of (top row) *meso*-hydroxy-dioxobacteriochlorin **10** (6.03×10^{-5} M) and dioxobacteriochlorin **7** (2.12×10^{-5} M) with tetrabutylammonium hydroxide (1 M in CH_3OH) in the [TBAOH] range indicated and (bottom row) of *meso*-hydroxy-dioxobacteriochlorin **10** (6.03×10^{-5} M) and dioxobacteriochlorin **7** (2.12×10^{-5} M) within the [TFA] ranges indicated.

ponding spectrophotometric titration of dioxobacteriochlorin **7** did not show any detectable changes, even after the addition of much higher concentrations of base.[15f]

Parallel to our interpretations of the findings for the deprotonation of *meso*-hydroxy-oxochlorin **9**, we attribute these findings to the deprotonation of the *meso*-hydroxy group in **10**. The deprotonation of the inner-core NH protons was not deemed feasible under these conditions. Accordingly, NMR titrations showed only the disappearance of the –OH proton signal (see ESI†). We also note that the deprotonated species were unstable over time under oxic conditions and attribute this to (irreversible) oxidations of the phenolate anion and the likely corresponding formation of a radical (see ESI†).

The protonation experiments (with TFA in CH_2Cl_2) are less dramatic but also clear-cut (Fig. 4): the spectral shifts observed upon protonation of free base **9** are much different from those of the non-hydroxylated species **6**,[15f] that also require significantly more acid for a protonation to take place. Nickel complex **9Ni** shows a qualitatively similar optical response to TFA. The combination of both findings suggests that protonation takes places at the peripheral oxygen atoms. A comparison of the computed optical spectra of **9** protonated at all possible O- and N-sites or of **9Ni** protonated at the oxo-functionality with the experimental spectra also confirms this interpretation (see ESI†).

Titration of *meso*-hydroxy-dioxobacteriochlorin **10** (6.03×10^{-5} M) with trifluoroacetic acid (TFA) resulted in the (reversible) formation of a much red-shifted and broadened longest wavelength band, along with a collapse of the intensity of the Soret band to under the absorbance of the Q-band (Fig. 5). This halochromic behaviour is fundamentally different from that of *meso*-hydroxy-oxochlorin **9** or its parent dioxobacteriochlorin **7**:[15f] upon protonation, the intensity of the prominent longest-wavelength Q-band erodes while the double Soret band of **7** shifts slightly into the blue. We interpret the unique protonation behaviour of **10** with the presence of two ketonic oxygen atom protonation sites that allow different resonance structures for the mono-cation to form.

Conclusions

The *meso*-OH-derivatized oxochlorins **9**, its nickel complex **9Ni**, and dioxobacteriochlorin **10** possess peripheral substitution patterns that suggest the presence of an acac-like moiety capable of binding metal ions, including the strong H-bond between the enol and flanking β-ketone. Like acac, the functionality can be deprotonated. However, unlike acac, we did not find any indication that this functionality is competent in chelating select 3d and 4d transition metal ions under the conditions tested. Evidently, the conjugation that contributes to the stability of acac as a ligand cannot be expressed in the *meso*-hydroxy-β-oxochlorins since the oxophlorin-like limiting resonance structure would perturb the aromaticity of the porphyrinic chromophores; likely, the metal binding energies do not offset the loss in aromaticity. The halochromic properties of the molecules provide some more insight into the location of the protonation/deprotonation sites, findings supported by computations. The facile formation of phenoxy radicals by the mono-anionic forms of these compounds is suggested.

Experimental section

Instrumentation

^{1}H NMR and ^{13}C NMR spectra were recorded using a Bruker AVANCE III 400 MHz spectrometer. IR spectra were recorded from neat material on a Bruker Alpha FTIR spectrometer using an attenuated total reflection (ATR) diamond crystal. Low- and high-resolution mass spectra were recorded in CH_3CN using AB Sciex API 2000 Triple Quadrupole and AB Sciex QStar Elite Quadrupole-TOF MS instruments, respectively. UV-Vis data were obtained on Varian Cary 100 or Cary 50 spectrophotometers; fluorescence spectra were recorded on a Cary Eclipse fluorimeter.

Crystals of **9Ni** or **10** were mounted on a Mitegen micromesh mount in a random orientation and data were collected from a shock-cooled single crystals at 150(2) K on a Bruker AXS D8 Quest four circle diffractometer with an I-mu-S microsource X-ray tube using a laterally graded multilayer (Goebel) mirror as monochromator and a PhotonIII_C14 charge-integrating and photon counting pixel array detector. The diffractometer used CuK$_\alpha$ radiation (λ = 1.54178 Å). All data were integrated with SAINT V8.40B and a multi-scan absorption correction using SADABS 2016/2 was applied.[27] The structures were solved by dual methods with SHELXT and refined by full-matrix least-squares methods against F^2 using SHELXL-2019/2.[28] All non-hydrogen atoms were refined with anisotropic displacement parameters. Carbon-bound H atoms, alcohol hydroxyl H atoms, and H atoms of planar (sp^2 hybridized) N–H groups were refined isotropically on calculated positions using a riding model. Methyl and hydroxyl H atoms were allowed to rotate but not to tip to best fit the experimental electron density. For water H atoms in **9Ni**, see ESI.† U_{iso} values were constrained to 1.5 times the U_{eq} of their pivot atoms for methyl and hydroxyl groups and 1.2 times for all other hydrogen atoms.

Additional data collection and refinement details, including a description of the disorder (where present), can be found in the ESI.†

Materials

Aluminum-backed, silica gel 60, 250 μm thickness analytical plates, glass-backed, 20 × 20 cm, 500 μm thickness silica gel 60 preparative TLC plates, and standard grade, 60 Å, 32–63 μm flash column silica gel were used for the separation/purification of the compounds.

Solvents and reagents were used as received. Octaethylporphyrin (**5**)[29] was made as described in the literature; it is also available from a number of chemical supply houses.

5-Hydroxy-7-oxo-octaethylchlorin (9)[20d]

Prepared in two steps from **5** in overall 25% yield (100 mg **5** scale) as described in the literature,[20d] except that instead of pure formic acid in the oxidation step, the porphyrin was dissolved in a minimal amount of CH_2Cl_2 before the fornic acid was added, with a final ratio of about 25% CH_2Cl_2/75% formic acid (90% aqueous solution). Spectroscopic data as described and reproduced for comparison in the ESI.†[20d]

[5-Hydroxy-7-oxo-octaethylchlorinato]nickel(II) (9Ni)

Free-base **9** (25 mg, 5.29 × 10^{-5} mol) was dissolved in toluene (20 mL) in a 50 mL round bottom flask. Ni(acac)$_2$ (68 mg, 2.65 × 10^{-4} mol, 5 equiv.) were added, and the reaction mixture was refluxed for 2 h. Reaction progress was monitored by thin-layer chromatography. After completion of the reaction, the solvent was removed under reduced pressure. The crude mixture was re-dissolved in CH_2Cl_2 (25 mL) and washed with deionized water to remove excess nickel salt. The organic layer was separated and dried over anhydrous Na_2SO_4 and the solvent removed under vacuum. The crude product was purified using column chromatography (silica gel/hexanes : CH_2Cl_2, 50 : 50 v/v) to yield **9Ni** as a green crystalline solid in 84% yield (23 mg, 3.68 × 10^{-5} mol). MW = 623.47 g mol^{-1}. R_f = 0.65 (silica-CH_2Cl_2 : hexanes, 2 : 1). ^{1}H NMR (400 MHz, $CDCl_3$): 12.93 (s, 1H, –OH), 9.11 (s, 1H, *meso*-H), 8.90 (s, 1H, *meso*-H), 8.18 (s, 1H, *meso*-H), 3.73 (q, $_3J^{H,H}$ = 7.4 Hz, 2H, –CH_2), 3.67–3.55 (m, 8H, –CH_2), 3.51 (q, $_3J^{H,H}$ = 7.6 Hz, 2H, –CH_2), 2.56–2.45 (m, 4H, –CH_2), 1.70–1.56 (m, 18H, –CH_3), 0.45 (t, $_3J^{H,H}$ = 7.4 Hz, 6H) ppm. ^{13}C{^{1}H} NMR (101 MHz, $CDCl_3$): 210.0, 154.0, 144.6, 144.3, 143.8, 143.4, 142.2, 142.1, 141.0, 140.5, 138.2, 137.1, 132.3, 122.0, 103.2, 96.4, 90.9, 63.1, 31.1, 21.5, 19.5, 19.3, 19.1, 18.4, 18.1, 17.9, 17.7, 16.7, 8.4 ppm. UV-vis (CH_2Cl_2) λ_{max} (log ε): 336 (4.23), 418 (4.76), 428 (4.75), 589 (3.94), 632 (4.30). IR (diamond ATR, neat): 1640 ($\nu_{C=O}$) cm^{-1}. HR-MS (ESI$^+$, 100% CH_3CN, TOF): calc'd for $C_{36}H_{44}N_4O_2Ni$ [M]$^+$ 622.2821, found 622.2725; calc'd for $C_{36}H_{43}N_4O_2Ni$ [M – H]$^{\bullet+}$ 621.2734, found 621.2686.

5-Hydroxy-7,17-dioxo-octaethylbacteriochlorin (10)

Prepared by H_2SO_4/H_2O_2-mediated oxidation of 7,17-dioxobacteriochlorin **7** (200 mg, 5.29 × 10^{-4} mol) and isolated as a minor product in 2% yield (6.2 mg, 1.06 × 10^{-5} mol) as purple solid powder.[21] Chromatographic condition: silica gel/hexanes–CH_2Cl_2 (30 : 70 v/v). MW = 582.789 g mol^{-1}. R_f = 0.677 (silica, CH_2Cl_2). ^{1}H NMR (400 MHz, $CDCl_3$): 13.60 (s, 1H, –OH), 8.97 (s, 1H, *meso*-H), 8.61 (s, 1H, *meso*-H), 8.47 (s, 1H, *meso*-H), 3.93 (q, 2H, $_3J^{H,H}$ = 7.4 Hz, 2H, –CH_2), 3.81–3.69 (m, 6H, –CH_2), 2.65–2.52 (m, 8H, –CH_2), 1.77–1.69 (dt, $_3J^{H,H}$ = 19.5, 7.5 Hz, 12H, –CH_3), 0.44 (dt, $_3J^{H,H}$ = 19.5, 7.5 Hz, 12H, –CH_3), −0.63 (d, $_3J^{H,H}$ = 25.9 Hz, 2H, –NH) ppm; ^{13}C{^{1}H} NMR (101 MHz, $CDCl_3$): 213.0, 210.8, 160.1, 158.9, 152.4, 145.4, 140.4, 140.0, 139.0, 138.5, 137.4, 135.3, 133.5, 131.3, 130.8, 128.8, 124.1, 95.7, 92.8, 88.7, 62.5, 58.5, 31.6, 58.5, 20.9, 18.3, 17.7, 17.4, 16.6, 8.5, 8.2, 1.0 ppm; UV-vis (CH_2Cl_2) λ_{max} (log ε): 410 (4.37), 578 (3.14), 600 (3.21), 626 (3.44), 677 (3.89) nm; fluorescence (CH_2Cl_2, $\lambda_{excitation}$ = 410 nm) $\lambda_{max\text{-}emission}$ = 683, 717 (sh) nm; FT-IR (diamond ATR, neat): 1709 ($\nu_{C=O}$), 3359 (ν_{N-H}) cm^{-1}; HR-MS (ESI$^+$, 100% CH_3CN, TOF): calc'd for $C_{36}H_{46}N_4O_3$ [M]$^+$ 582.3570, found 582.3525; calc'd for $C_{36}H_{47}N_4O_3$ [M + H]$^+$ 583.3643, found 583.3589.

Author contributions

NC did the investigation, data curation, visualization, and analysis, wrote the first draft, reviewed & edited the final draft. MJG-P: Performed all computations and contributed to data analysis and visualization. MZ performed single crystal diffractometry analyses. CB was involved in the conceptualization, data analysis and visualization, funding acquisition, project administration, writing, review & editing of the final manuscript with input from all authors.

Data availability

The data underlying this study are available in the published article and its ESI.†

Crystallographic data for **9Ni** and **10** have been deposited at the CCDC under 2340919–2340920.†

ESI data available: Reproductions of all spectra (UV-vis, Fl, ^{1}H, ^{13}C NMR spectra, FT-IR, MS spectra) of **10**; spectroscopic data of known compound **9** for comparison; details to the single crystal X-ray structure analyses; graphical representations of the computational data, including movies of trajectories; computational datasets.

Conflicts of interest

There are no conflicts to declare.

Acknowledgements

This work was supported by the US National Science Foundation under Grant Number CHE-1800361 (to CB) and CHE-1625543 (to MZ). M. J. G.-P. wishes to acknowledge the financial support of an Office of Vice Provost Research fellowship at Baylor University. We thank Chi-Kwong (Chris) Chang, Michigan State University, for donation of the OEP used in this study.

References

1 (*a*) B. Bock, K. Flatau, H. Junge, M. Kuhr and H. Musso, *Angew. Chem., Int, Ed. Engl.*, 1971, **10**, 225–235; (*b*) C. Pettinari, F. Marchetti and A. Drozdov, in *Comprehensive Coordination Chemistry II*, ed. J. A. McCleverty and T. B. Meyer, Pergamon Press, Oxford, 2003, vol. 1, pp. 97–116; (*c*) V. V. Skopenko, V. M. Amirkhanov, T. Y. Sliva, I. S. Vasilchenko, E. L. Anpilova and A. D. Garnovskii, *Russ. Chem. Rev.*, 2004, **73**, 737–752; (*d*) A. S. Crossman and M. P. Marshak, in *Comprehensive Coordination Chemistry III*, ed. E. C. Constable, G. Parkin and J. Lawrence Que, Elsevier, Oxford, 2021, vol. 1, pp. 331–365.

2 G. de Gonzalo and A. R. Alcántara, *Pharmaceuticals*, 2021, **14**, 1043.

3 P. Dandawate, S. Padhye, R. Schobert and B. Biersack, *Expert Opin. Drug Discovery*, 2019, **14**, 563–576.

4 (*a*) A. Alka, V. S. Shetti and M. Ravikanth, *Coord. Chem. Rev.*, 2019, **401**, 213063; (*b*) D. W. Thuita and C. Brückner, *Chem. Rev.*, 2022, **122**, 7990–8052.

5 (*a*) J. W. Buchler, in *The Porphyrins*, ed. D. Dolphin, 1978, vol. 1, pp. 389–483; (*b*) C. J. Kingsbury and M. O. Senge, *Coord. Chem. Rev.*, 2021, **431**, 213760.

6 K. Pyrzynska, K. Kilian and M. Pęgier, *Molecules*, 2022, **27**, 3311.

7 S. Richeter, J. Christophe, G. Jean-Paul and R. Romain, in *Handbook of Porphyrin Science*, ed. K. M. Kadish, K. M. Smith and R. Guilard, World Scientific Publishing Company, Hackensack, NJ, 2010, vol. 3, pp. 429–483.

8 B. Szyszko and L. Latos-Grazynski, *Chem. Soc. Rev.*, 2015, **44**, 3588–3616.

9 S. Richeter, C. Jeandon, J.-P. Gisselbrecht, R. Graff, R. Ruppert and H. J. Callot, *Inorg. Chem.*, 2004, **43**, 251–263.

10 A. Srinivasan, H. Furuta and A. Osuka, *Chem. Commun.*, 2001, 1666–1667.

11 (*a*) M. C. A. F. Gotardo, H. C. Sacco, J. C. S. Filho, A. G. Ferreira, A. C. Tedesco and M. D. Assis, *J. Porphyrins Phthalocyanines*, 2003, **7**, 399–404; (*b*) L. Poyac, C. Rose, M. Wahiduzzaman, A. Lebrun, G. Cazals, C. H. Devillers, P. G. Yot, S. Clément and S. Richeter, *Inorg. Chem.*, 2021, **60**, 19009–19021; (*c*) H. Mansour, M. E. El-Khouly, S. Y. Shaban, O. Ito and N. Jux, *J. Porphyrins Phthalocyanines*, 2007, **11**, 719; (*d*) N. A. Le, V. Babu, M. Kalt, L. Schneider, F. Schumer and B. Spingler, *J. Med. Chem.*, 2021, **64**, 6792–6801; (*e*) A. B. Becceneri, M. T. Martin, A. E. Graminha, M. R. Cominetti, P. C. Ford and R. Santana da Silva, *Dalton Trans.*, 2024, **53**, 11264–11275.

12 Y. Ding, W.-H. Zhu and Y. Xie, *Chem. Rev.*, 2017, **117**, 2203–2256.

13 (*a*) J.-C. Chambron, V. Heitz and J.-P. Sauvage, in *The Porphyrin Handbook*, ed. K. M. Kadish, K. M. Smith and R. Guilard, Academic Press, San Diego, CA, 2000, vol. 6, pp. 1–42; (*b*) V. S. Shetti, Y. Pareek and M. Ravikanth, *Coord. Chem. Rev.*, 2012, **256**, 2816–2842.

14 J. Wojaczynski and L. Latos-Grazynski, *Coord. Chem. Rev.*, 2000, **204**, 113–171.

15 (*a*) H. H. Inhoffen and W. Nolte, *Justus Liebigs Ann. Chem.*, 1969, **725**, 167–176; (*b*) M. Liu, C.-Y. Chen, D. Hood, M. Taniguchi, J. R. Diers, D. F. Bocian, D. Holten and J. S. Lindsey, *New J. Chem.*, 2017, **41**, 3732–3744; (*c*) D. Hood, D. M. Niedzwiedzki, R. Zhang, Y. Zhang, J. Dai, E. S. Miller, D. F. Bocian, P. G. Williams, J. S. Lindsey and D. Holten, *Photochem. Photobiol.*, 2017, **93**, 1204–1215; (*d*) M. Taniguchi, H.-J. Kim, D. Ra, J. K. Schwartz, C. Kirmaier, E. Hindin, J. R. Diers, S. Prathapan, D. F. Bocian, D. Holten and J. S. Lindsey, *J. Org. Chem.*, 2002, **67**, 7329–7342; (*e*) M. E. Alberto,

B. C. De Simone, E. Sicilia, M. Toscano and N. Russo, *Int. J. Mol. Sci.*, 2019, **20**, 2002; (*f*) D. Schnable, N. Chaudhri, R. Li, M. Zeller and C. Brückner, *Inorg. Chem.*, 2020, **59**, 2870–2880.

16 (*a*) C. K. Chang, *Biochemistry*, 1980, **19**, 1971–1976; (*b*) C. Brückner, N. Chaudhri, D. E. Nevonen, S. Bhattacharya, A. Graf, E. Kaesmann, R. Li, M. J. Guberman-Pfeffer, T. Mani, A. Nimthong-Roldán, M. Zeller, A. A. P. Chauvet and V. Nemykin, *Chem. – Eur. J.*, 2021, **27**, 16189–16203.

17 (*a*) H. Fischer and H. Orth, *Die Chemie des Pyrrols*, Akademische Verlagsgesellschaft (Johnson Reprint, New York 1968), Leipzig, 1937; (*b*) H. Fischer, H. Gebhardt and A. Rothhaas, *Justus Liebigs Ann. Chem.*, 1930, **482**, 1–24.

18 (*a*) R. Bonnett, D. Dolphin, A. W. Johnson, D. Oldfield and G. F. Stephenson, *Proc. Chem. Soc.*, 1964, 371–372; (*b*) R. Bonnett, M. J. Dimsdale and G. F. Stephenson, *J. Chem. Soc. C*, 1969, 564–570; (*c*) H. H. Inhoffen and W. Nolte, *Tetrahedron Lett.*, 1967, **8**, 2185–2187.

19 (*a*) A. M. Stolzenberg and M. T. Steshic, *J. Am. Chem. Soc.*, 1988, **110**, 6391–6402; (*b*) R. Bonnett, A. N. Nizhnik and M. C. Berenbaum, *J. Chem. Soc., Chem. Commun.*, 1989, 1822–1823; (*c*) C. K. Chang, K. M. Barkigia, L. K. Hanson and J. Fajer, *J. Am. Chem. Soc.*, 1986, **108**, 1352–1354; (*d*) K. M. Barkigia, C. K. Chang, J. Fajer and M. W. Renner, *J. Am. Chem. Soc.*, 1992, **114**, 1701–1707; (*e*) D. B. Papkovsky, G. V. Ponomarev, W. Trettnak and P. O'Leary, *Anal. Chem.*, 1995, **67**, 4112–4117; (*f*) T. J. Neal, S.-J. Kang, I. Turowska-Tyrk, C. E. Schulz and W. R. Scheidt, *Inorg. Chem.*, 2000, **39**, 872–880; (*g*) F. Tutunea and M. D. Ryan, *J. Electroanal. Chem.*, 2012, **670**, 16–22; (*h*) R. Li, M. Zeller and C. Brückner, *Eur. J. Org. Chem.*, 2017, 1820–1825; (*i*) R. Li, M. Zeller and C. Brückner, *J. Porphyrins Phthalocyanines*, 2018, **22**, 562–572; (*j*) N. Chaudhri, M. Zeller and C. Brückner, *J. Org. Chem.*, 2020, **85**, 13951–13964; (*k*) S. Bhattacharya, A. Graf, A. K. M. S. Gomes, N. Chaudhri, D. Chekulaev, C. Brückner, T. M. Cardozo and A. A. P. Chauvet, *J. Phys. Chem. A*, 2022, **126**, 2522–2531; (*l*) S. Bhattacharya, D. E. Nevonen, A. J. Auty, A. Graf, M. Appleby, N. Chaudhri, D. Chekulaev, C. Brückner, A. A. P. Chauvet and V. N. Nemykin, *J. Phys. Chem. A*, 2023, **127**, 7694–7706.

20 (*a*) H. H. Inhoffen and A. Gossauer, *Justus Liebigs Ann. Chem.*, 1969, **723**, 135–148; (*b*) M. Isaac, M. O. Senge and K. M. Smith, *J. Chem. Soc., Perkin Trans. 1*, 1995, 705–714; (*c*) E. Meehan, R. Li, M. Zeller and C. Brückner, *Org. Lett.*, 2015, **17**, 2210–2213; (*d*) R. Li, E. Meehan, M. Zeller and C. Brückner, *Eur. J. Org. Chem.*, 2017, 1826–1834; (*e*) R. Li, M. Zeller, T. Bruhn and C. Brückner, *Eur. J. Org. Chem.*, 2017, 1835–1842.

21 N. Chaudhri, M. J. Guberman-Pfeffer, R. Li, M. Zeller and C. Brückner, *Chem. Sci.*, 2021, **12**, 12292–12301.

22 S. S. Sano, T. Morishima, I. Shiro and Y. Maeda, *Proc. Natl. Acad. Sci. U. S. A.*, 1986, **83**, 531–535.

23 (*a*) P. S. Clezy, in *Porphyrins*, ed. D. Dolphin, Academic Press, NY, 1978, vol. 2, pp. 103–130; (*b*) M. J. Crossley, L. G. King and S. M. Pyke, *Tetrahedron*, 1987, **43**, 4569–4577; (*c*) L. Szterenberg, L. Latos-Grazynski and J. Wojaczynski, *ChemPhysChem*, 2002, **3**, 575–583.

24 M. O. Senge and K. M. Smith, *J. Chem. Soc., Chem. Commun.*, 1992, 1108–1109.

25 G. A. Jeffrey, *An introduction to hydrogen bonding*, Oxford University Press, New York, 1997.

26 (*a*) P. R. Dongare and A. H. Gore, *ChemistrySelect*, 2021, **6**, 5657–5669; (*b*) X. Zheng, W. Cheng, C. Ji, J. Zhang and M. Yin, *Rev. Anal. Chem.*, 2020, **39**, 231–246; (*c*) K. P. Carter, A. M. Young and A. E. Palmer, *Chem. Rev.*, 2014, **114**, 4564–4601.

27 (*a*) *Bruker, SAINT, V8.40A*, Bruker AXS Inc., Madison, Wisconsin, USA; (*b*) L. Krause, R. Herbst-Irmer, G. M. Sheldrick and D. Stalke, *J. Appl. Crystallogr.*, 2015, **48**, 3–10.

28 (*a*) G. M. Sheldrick, *Acta Crystallogr., Sect. A: Found. Crystallogr.*, 2008, **A64**, 112–122; (*b*) G. M. Sheldrick, *Acta Crystallogr., Sect. C: Struct. Chem.*, 2015, **71**, 3–8.

29 (*a*) J. B. Paine III, W. B. Kirshner, D. W. Moskowitz and D. Dolphin, *J. Org. Chem.*, 1976, **41**, 3857–3860; (*b*) J. L. Sessler, A. Mozaffari and M. R. Johnson, *Org. Synth.*, 1992, **70**, 68–78; (*c*) C. B. Wang and C. K. Chang, *Synthesis*, 1979, 548–549.

